Desalination and Water Treatment
www.deswater.com

doi:10.5004/dwt.2019.23167

139 (2019) 156–165
January

The adsorptive potential of graphene monolith for organic pollutant treatment: kinetics, isotherms, and thermodynamics of interactions

Asif Hussain, Tallal Bin Aftab, Guo Qihao, Jiebing Li, Dengxin Li*

School of Environmental Science and Engineering, Donghua University Shanghai- 201620, China, Tel. +86-13122194207, email: asif.fuuast@hotmail.com (A. Hussain), Tel. +86-13122174017, email: tallal@live.com (T. Bin-Aftab), Tel. +86-13122174017, email: 958937911@qq.com (Q. Guo), Tel. +86-18817334012, email: 576115487@qq.com (J. Li), Tel. +86-2167792541, Fax + 86-2167792522, email: lidengxin@mail.dhu.edu.cn (D. Li)

Received 26 March 208; Accepted 17 September 2018

ABSTRACT

Nano-scale graphene has been employed to remove dye pollutants in wastewater treatment. However, engineering concerns associated with inconvenient recollection of nano-graphene and bio-toxicity to human cells significantly hampered its application for environmental protection. In this study, monolithic form of graphene was fabricated by urea assisted self-assembly protocols and applied as an adsorbent to remove model organic pollutant, methylene blue dye (MB). The fabricated material was characterized by scanning electron microscopy (SEM), Fourier transmission infrared spectroscopy (FT-IR), Raman spectroscopy, and X-ray photo electron spectroscopy (XPS), Thermogravimetric analysis (TGA) and nitrogen adsorption-desorption isotherms. Characterization results show that graphene monolith with tailored macroscopic dimension, highly porous network and active binding sites (e.g., functional groups and aromatic domains) could provide facile mass transfer of pollutant and cost-effective recollection. Adsorptive removal of MB best suited to Langmuir isotherm, pseudo-second-order kinetics, and intra particle diffusion kinetics models. Complete removal of MB (>98%) was achieved under optimum conditions (e.g., alkaline pH, 160 mM of salt and 1 g/L adsorbent dose at 25°C). Removal of MB using monolith was favorable, spontaneous and exothermic adsorption process. Electrostatic and π-π staking interactions were identified as major interaction process. A monolithic form of graphene demonstrates the advantageous potential for the safe and efficient treatment of environmental pollutants.

Keywords: Monolithic graphene; Adsorption; Interaction mechanism; Organic pollutant

1. Introduction

The world wide discovery of synthetic dyes now recorded a global annual production of >800,000 tons for various industrial applications [1]. Among them, the textile industry uses more than 10,000 of different dyes with annual consumption of 7×10^5 tons, and indeed a prevalent source of wasted dye discharged into a water bodies that cause a serious water pollution issue [1,2]. Specifically, dyes can impart unaesthetic color and reduced the sunlight penetration into water bodies, resulting in undesirable impacts on water use (e.g., human consumption) and photochemical activities of aquatic life [3]. They can degrade into toxic compounds which have carcinogenic or mutagenic effects on living organisms [4]. As an essential basic dye for printing calico, dyeing cotton and lather, methylene blue (MB) could cause serious health concerns (e.g., increase heart rate, cyanosis, vomiting, jaundice, gastritis, mental confusion,and methemoglobinemia) [5]. Furthermore, dyes used in the textile industry generally possess high stability against chemical,sunlight and microbial attack. Therefore, biodegradation or biological treatment of such dyes are very difficult, time-consuming and ineffective [6]. Hence, it is imperative that suitable treatment techniques should be devised. Among various

*Corresponding author.

treatment techniques, adsorption of organic dyes exhibits manifold advantage such as efficient phase transfer of dye pollutants onto adsorbent without producing fore seen toxic intermediates, insensitive to toxic compounds, easiness of operation, cost-efficient, and simplicity of design [6–12]. Removal of dye pollutants (e.g., MB) using various forms of activated carbons have extensively employed as an important application of adsorption process [1,9–11]. However, engineering concerns associated with high-cost calcination and environmental concerns associated with the release of toxic pollutant during synthesis of activated carbon significantly limits its use as an adsorbent.

Discovery of graphene, the two-dimensional carbon nanomaterial comprising a single layer of sp^2 carbon atoms arranged in a hexagonal ring, emerged as an efficient and low-cost alternative for MB adsorption [13]. The sizeable theoretical surface area (2630 g/m^2) [14], oxygen functional groups (e.g. carboxylate and latcols) on the edge of graphene and sp^2-hybridized graphene domains on the basal plan along with some epoxy and hydroxyl groups, motivated worldwide resurgence of synthesis, characterization and application of graphene-based adsorbents [11,15–20]. However, engineering concerns associated with nano-scale graphene (i.e., inconvenient recovery and high-cost post-treatment) and insufficient phase transfer of pollutant molecules associated with staking aggregation of graphene sheets limits its application.

Alternatively, efforts have been made to integrate the graphene nano-building units into a highly porous macroscopic material (e.g., generally refer as monolith or sponge or foam) through scalable self-assembly protocols [13,21,22]. The surface morphology and functionality of self-assembled graphene can be manipulated using modifiers and reducing agents for the decontamination of organic pollutants from water. For instance, Zhao et al. use thiourea based highly functional graphene sponge for the treatment of dye rhodamine B [14]. Tiwari et al., applied sodium ascorbate to assembled graphene hydrogel for the removal of MB [23]. Li et al. fabricated luffa based graphene sponge to remove cationic dyes [24]. Shi et al. assembled three dimensional graphene using glutathione and liquid ammonia for the removal of malachite green dye [25]. It was further showed that sponge-like graphene fabricated by melamine [26], and ammonia [27] can efficiently remove organic oil pollutants from waters. To the best of our knowledge, there is no report available on the comprehensive adsorption dynamics of MB dye using urea based graphene monolith. In this study, adsorptive potential of graphene monolith systematically investigated for the removal of MB dye under various operating conditions. Batch adsorption data used to stablish adsorption isotherm, kinetics, thermodynamics, and modeling of interaction. Below are the details of research work.

2. Experimental

2.1. Materials

Flake of natural graphite (300 mesh size, ≥ 99%) obtained from Shanghai Yifan Graphite, China. Sodium nitrate ($NaNO_2$, ≥ 99%), potassium permanganate ($KMnO_4$), sulfuric acid (H_2SO_4, 98%), hydrogen peroxide (H_2O_2, 30%), hydrochloric acid (HCl, 36%) supplied by Sino-pharm chemical and reagent, China. Urea (NH_2CONH_2, ≥ 99%) and methylene blue dye (MB, $C_{16}H_{18}ClN_3S$, MW = 319.86) purchased from Sigma-Aldrich.

2.2. Synthesis of graphene oxide

Graphene oxide (GO) synthesized by reported chemical oxidation protocols [28]. First, 5 g of graphite powder mixed with 2.5 g of sodium nitrate and 115 ml of concentrated sulfuric acid (H_2SO_4, 98%).The mixture was cool to 4°C over an ice bath, and then 15 g of potassium permanganate ($KMnO_4$) was gradually added into the reaction mixture and set at constant stirring for two h. Next, the temperature of the slurry was first raised to 35°C and reacted for two h then 230 ml of distilled water was added, and temperature of the reaction mixture was further raised to 98°C and reacted for 15 min to complete oxidation process. Finally, the reaction mixture was diluted with 700 ml of distilled water and immediately quenched with 50 ml of hydrogen peroxide (H_2O_2, 30%) upon which the sand color product obtained. The product was purified by washing with HCl (1:10, 500 ml) and deionized water until pH = 5–6. The purified product was centrifuged (12000 rpm), freeze drying and labeled as GO for further use.

2.3. Fabrication of graphene monolith

Monolith of graphene was fabricated by urea assisted self-assembly protocols (Fig. 1). In a typical synthesis, 200 mg of graphene oxide was homogeneously dispersed in 100 ml of deionized water using tip sonication. Next, 400 mg of urea added to graphene suspension and mixed well-using stirrer. After that, the 30 ml of the mixture was immediately sealed in the Teflon-lined stainless steel hydrothermal reactor and placed in an oven at 180°C for 5 h. Finally, the black color graphene monolith was recovered from the reactor and dipped into distilled water for 24 h to remove residual impurities. The product was freeze dry and used for further characterization.

2.4. Characterization

Micro structure morphology monolith was analyzed by S420 scanning electron microscopy (Hitachi, Japan). Surface chemistry of sample was investigated by Fourier transforms infrared spectroscopy (FT-IR) using 6700 spectrophotometer (Nicolet, UK) and X-ray photo electron spectroscopy (XPS) on a XI250 Escalab system (Thermo Fisher, England). Raman analysis was performed on a Nexus 670 Raman spectrometer (Renishaw, USA). BET surface area and BJH pore distribu-

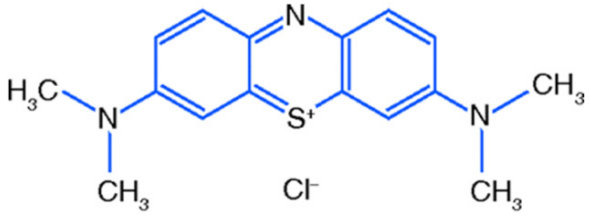

Fig. 1. Chemical structure of methylene blue dye (MB).

tion curves obtained from nitrogen adsorption-desorption isotherms using a Micromeritics Tristar II 3020 surface area analyzer (Norcross, GA). Zeta potential measurement (Z.P) was carried out by Nano-ZS90 Zetasizer. Thermal property of the monolith was tested by a TG-209F1 thermogravimetric analyzer (Netzsch, Germany) in a nitrogen environment over temperature range of 30–900°C and heating rate of 10°C/min. Solution pH was adjusted by 0.1 M HCl or NaOH and monitored by a Mettler Toledo FG2 pH meter (USA).

2.5. Dye adsorption study

Adsorption performance of graphene monolith was examined by model organic dye methylene blue, MB (Fig. 2). The known quantity of graphene monolith added into a desired concentration of MB solution at neutral pH and temperature of 25°C. Next, 3 ml of sample was withdrawn after a predetermined time, and residual concentration of MB immediately analyzed by UV-1800 spectrophotometer (Shimadzu, Japan) at absorbance maximum (λ_{max} = 664 nm). The experimental data obtained from the effect of contact time, MB concentration, pH, sodium chloride and temperature were used to calculate adsorption quantity and removal percentage of MB using Eqns. (1) and (2), respectively.

$$q_e = \frac{(C_o - C_e)V}{m} \tag{1}$$

$$\%\,Removal = \frac{C_o - C_t}{C_o} \times 100 \tag{2}$$

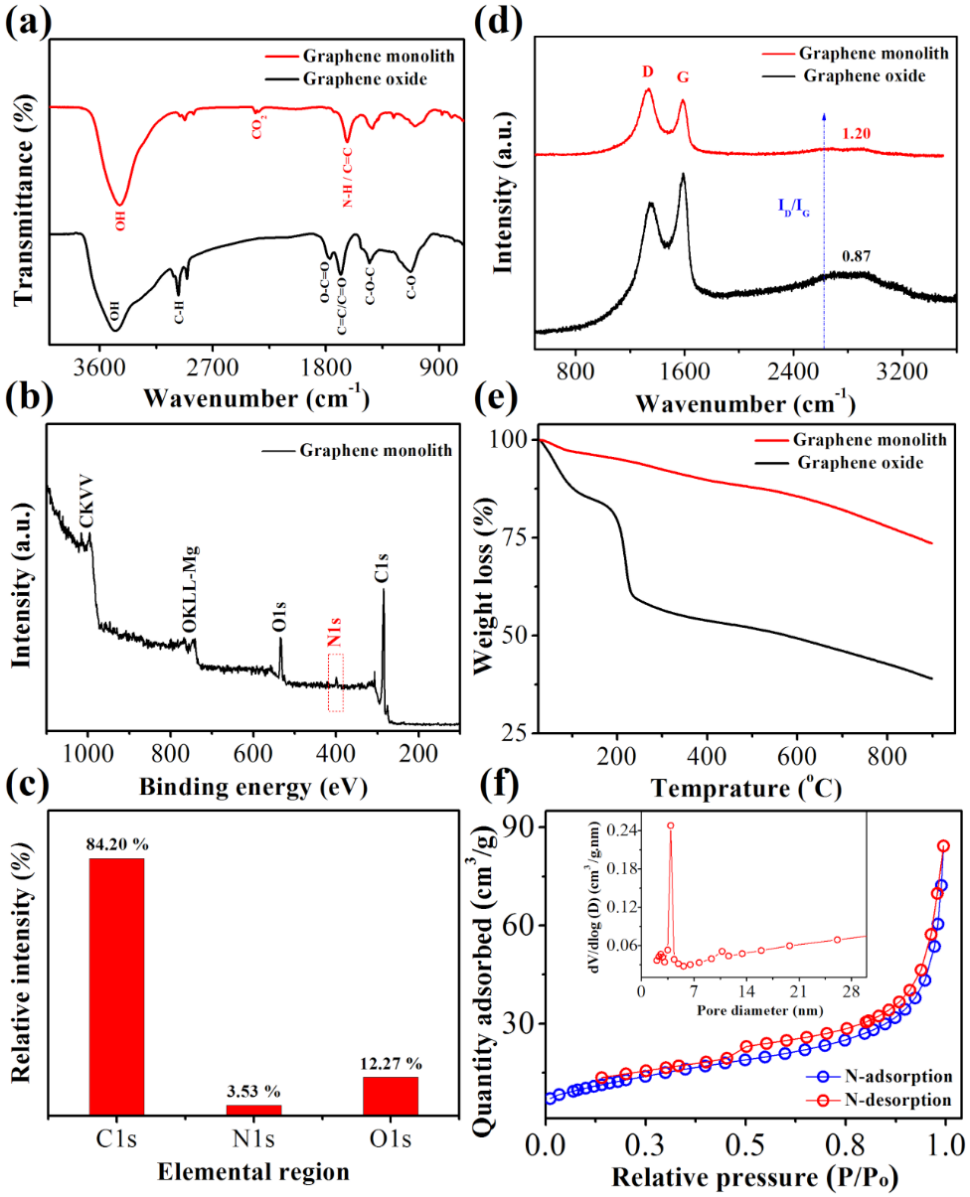

Fig. 2. FT-IR spectra (a), X-ray photo electron survey spectrum (b), elemental composition of monolith (c), Raman spectra (d), thermogravimetric curves (e) and nitrogen adsorption-desorption isotherms (f).

where q_e is the quantity of MB adsorbed in mg/g at equilibrium. C_o and C_e represent initial and the equilibrium concentration of MB dye in mg/l respectively. V and m represents the volume of MB solution in liter and added the amount of monolith adsorbent in gram.

3. Results and discussion

3.1. Characterization of the monolith

Physiochemical properties were obtained to evaluate the surface chemistry and morphology of the fabricated graphene monolith. From Fig. 2a, FTIR spectrum of GO indicates the various oxygen functional groups such as hydroxyl (OH) at 3400 cm^{-1}, carboxyl (O-C=O) at 1720 cm^{-1}, carbonyl (C=O) at 1627 cm^{-1}, alkoxy (C-O-C), at 1240 cm^{-1} and epoxy (C-O) at 1047 cm^{-1}. Compare to GO; monolith spectrum undergoes significant changes upon urea assisted self-assembly treatment such as the disappearance of carboxyl band located at 1720 cm^{-1}, shifting and shrinkage of hydroxyl band at 3400 cm^{-1} and newly appeared band at 1631 cm^{-1} arising from N–H bending vibration. Taking together FTIR results confirmed the formation of chemical bonds (e.g., amide and intra molecular hydrogen bonding) and reduction of graphene oxide during self-assembly process. This speculation was further confirmed by XPS elemental survey results which revealed the presence of nitrogen and oxygen functional groups on the surface of graphene monolith (Fig. 2b). The surface atomic ratio of the monolith was in the order of: carbon (1Cs = 84.20%)> oxygen content (O1s = 12.27%) > nitrogen (1Ns = 3.53%), indicating the existence of active functional groups and partially reduced graphene forms (Fig. 2c). Raman spectrum of graphene oxide showed two characteristics bands located at 1356 and 1591 cm^{-1} corresponding to disorder D-band (Sp^3 hybridized) and order G-band (Sp^2 hybridized) with an intensity ratio of I_D/I_G = 0.87. In contrast, the spectrum of graphene monolith undergoes a not able change in the intensity ratio (i.e., I_D/I_G = 1.20) and D band grown in intensity upon urea assisted treatment (Fig. 2d). These results confirmed that the fabricated monolith possesses a higher density of crystalline graphene regions (i.e., reduced form) compare to amorphous counterparts (i.e., GO). Thermal stability of monolith examined by thermogravimetric curves (TGA) analysis (Fig. 2e). The TGA curve of graphene oxide showed the minor weight loss at ≅ 100°C due to dehydration of adsorbed water molecules [29].

After that, GO curve exhibited degradation with an onset temperature of 198°C and mass loss of 20% due to the removal of oxygen functional groups from GO back bones. In contrast, the monolith curve showed enhanced thermal stability as a result of the bonding interaction between oxygen functional groups of graphene and urea intermediates, also agree with FTIR and Raman spectra results. Furthermore, the surface charge of the monolith was measured by zeta potential analyzer and found to be –27.93 ± 0.66. Taking together, the chemical analysis suggests that fabricated monolith is thermally stable and contain sufficient negative charge surface and active adsorptive sites (i.e., oxygen and a mine functional groups, and aromatic C=C of graphene domains).

Surface morphology of the monolith is shown in Fig. 3. The inset digital image showed that a monolithic form of graphene with tailored macroscopic dimensions could easily obtain through urea assisted self-assembly protocols (inset Fig. 3a). This result suggests that urea can behave like a strong binding agent between graphene sheets, resulting in the formation of monolith material. Low magnification SEM image showed a 3D network of multi-dimensional pores similar to the sponge-like material (Fig. 3a). Upon magnification 3D morphology remained and showed serval creased or wrinkled on the surface of graphene monolith (Fig. 3b). Nitrogen adsorption-desorption isotherm analysis further investigated for pores structures. The shape of isotherm exhibited type-IV isotherm, a typical signature of material consisting of mesopores and micro pores (Fig. 3f). The small opening at high relative pressure (P/P_o = 0.5–0.8) indicates the type H_3 nature of hysteresis loops, which suggest the cylindrical-like pores [30]. Barrett-Joyner-Halenda (BJH) curve also confirms the distribution of pores in mesoporous reigns (inset Fig. 3f). The BET surface area, average pore diameter and pore volume of the monolith were measured as 48.15 m^2/g, 10.6 nm, and 1.34 cm^3/g respectively. All these results demonstrate favorable adsorption properties of monolith such as facile recollection, sufficient mesoporous porosity and active adsorption sites (i.e., creased or wrinkled) for MB adsorption.

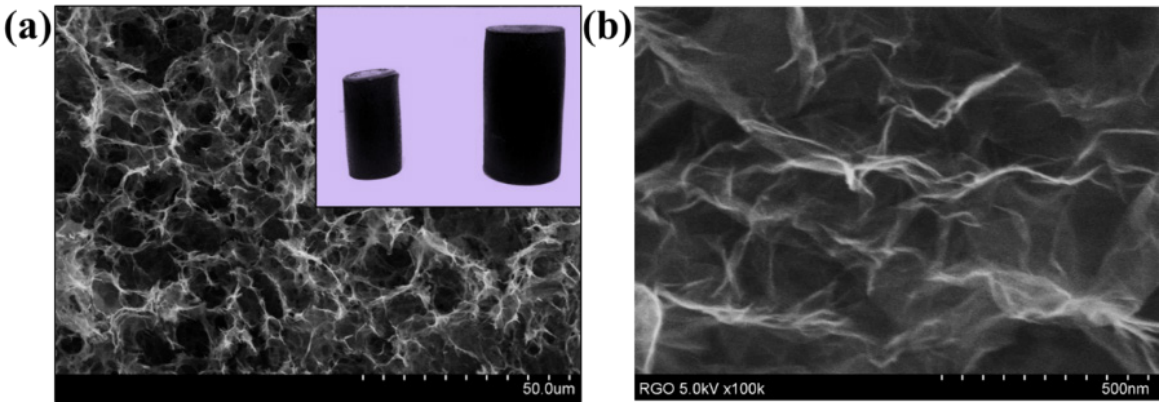

Fig. 3. SEM images of graphene monolith, low magnification (a) and high magnification (b).

3.2. Adsorption performance of monolith

The adsorbent dose is an essential parameter of the adsorption process and gives information about the performance of adsorbent at a particular concentration of dye solution. Fig. 4a shows the effect of adsorbent dose and contact time for MB removal using variable adsorbent dose (i.e., 0.01–0.05 g), constant pH of 6.7, MB concentration of 30 mg/l and temperature of 25°C. It can be seen that removal of MB increased as more dosage of the monolith was used. A substantial increase in MB removal rate occurs (i.e., from 35% to 98%) upon increasing adsorbent dose from 0.01g to 0.05 g. This result indicates that more massive adsorbent dose provides more binding sites for the fixed number of MB molecules. Thus the amount of monolith held at 0.05 g (1.0 g/l) in all subsequent kinetics and sorption studies. Further, the adsorbent to MB ratio also showed an increased removal of MB with contact time. The MB removal efficiency of the monolith was quite rapid within the first 90 min of contact followed by slowly approached equilibrium. Saturation reached after 300 min of contact time. This result suggests that a large number of vacant adsorptive sites were available and rapidly occupied at initial stage then attained repulsive force between remaining MB molecules and adsorbent surface in the solution.

3.3. Adsorption kinetics

Adsorption kinetics provides the information about the rate controlling mechanisms of adsorption process such as mass transfer and chemical interaction. MB adsorption data obtained for studied initial concentrations of MB dye (30 and 50 mg/l) using 0.05 g of monolith dose at a constant pH of 6.7 and temperature of 25°C. Experimental data of MB adsorption applied to linearized forms of pseudo-first-order and pseudo-second-order kinetics Eqns. (3) and (4), respectively [5,6].

$$\log(q_e - q_t) = \log(q_e) - \frac{k_1 t}{2.303} \tag{3}$$

$$\frac{t}{q_t} = \frac{1}{k_2 (q_e)^2} + \frac{t}{q_e} \tag{4}$$

where q_e and q_t are the amounts of dye MB (mg/g) adsorbed onto monolith at equilibrium and at time t (min) respectively, whereas k_1 (1/min) and k_2 (g/mg/min) is the rates constant of pseudo-first-order and pseudo-second-order of the adsorption process. Figs. 4b and 4c show pseudo-first-order and pseudo-first-order plot for MB adsorption data. The coefficient of determination (r^2) and rate constant value of k_1 and k_2 for studied MB initial concentration are presented in Table 1. It can be seen that the plot of pseudo-second-order gives excellent fitting of experimental data compare to pseudo-first-order kinetics. Furthermore, the comparatively higher value of $r^2 = 0.996$ and minimal deviation of MB equilibrium adsorption capacity (q_e) between calculated and experimental values indicate that the adsorption of MB followed pseudo-second-order kinetics and may govern by chemisorption process.

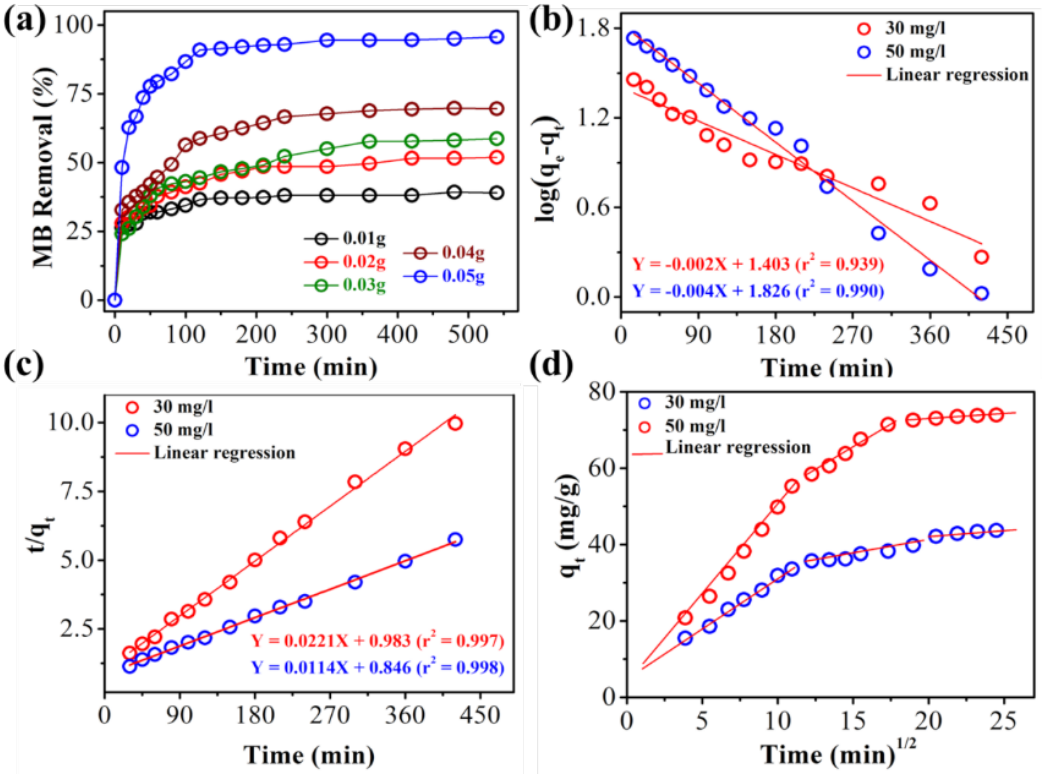

Fig. 4. Effect of adsorbent dosage (a), pseudo-first-order kinetic model (b), pseudo-second-order kinetic model (c), and intra particle diffusion kinetic model (d) for the removal of MB.

Table 1
Estimated kinetics parameters for the removal of MB dye

C_o of MB (mg/l)	Pseudo-first-order kinetics			Pseudo-second-order kinetics			$q_{e,(exp.)}$ (mg/g)
	k_1 (min^{-1})	$q_{e'(calculated)}$ (mg/g)	R^2	k_2 (min^{-1})	q_{ecal} (mg/g)	R^2	
30	0.00576	25.29	0.944	0.00055	44.64	0.997	44.01
50	0.01013	67.11	0.991	0.00017	85.47	0.996	74.11

3.4. Mass transfer analysis

For a solid-liquid sorption process, the solute transfer generally comprises on the multi step processes such as external mass transfer, intra particle diffusion (e.g., internal diffusion of adsorbate onto the pore wall of adsorbent) or both. The kinetics data were further analyzed by Weber and Morrie intra particle diffusion model using Eq. (5) [31].

$$q_t = k_{ip} t^{1/2} + C \tag{5}$$

where q_t is the adsorption capacity of monolith at time t (mg/g), k_{ip}(mg/g $min^{1/2}$) is the intra particle diffusion rate constant, "t" is time (min) and C (mg/g) is the thickness of boundary layer for adsorption steps. Fig. 4d shows that adsorption of MB onto graphene monolith comprises on multi-step adsorption processes for both investigated concentration of MB since it did not pass through the origin (C≠0). From Table 2, the first stage represents the boundary layer diffusion of MB molecules from the bulk solution to the external surface of the monolith. The broader rate constant values (k_{id} = 2.648 and 4.948 mg/g $min^{1/2}$) and lower C value (5.07 and 0.17 mg/g) indicated the rapid adsorption of MB through film/surface diffusion process due to sufficient binding sites of graphene monolith. The second phase of adsorption showed a sharp decline in k_{id} value (0.619 and 2.266 mg/g $min^{1/2}$) and significantly larger C value (27.76 and 31.19 mg/g) compare to film/surface diffusion step. These results suggest the gradual diffusion of MB molecules into multi-pores of monolith where intra particle diffusion was rate-limiting step [31]. Finally, adsorption of MB extremely slowdown and approached to equilibrium stage and thoroughly agree with the highest C values of the third stage (e.g., 34.29 and 78.72 mg/g). The diffusion kinetics results demonstrate that film/surface and intra particle diffusion mechanisms were both rates limiting adsorption processes for the removal MB dye.

Table 2
Intra particle diffusion model parameters for the removal of MB dye

Diffusion Phases	C_o = 30 mg/l			C_o = 50 mg/l		
	k_{ip}	C (mg/g)	R^2	k_{ip}	C (mg/g)	R^2
Film/surface	2.648	5.07	0.983	4.948	0.17	0.995
Intra particle	0.619	27.76	0.953	2.266	31.19	0.940
Equilibrium	0.387	34.31	0.974	0.215	68.72	0.943

3.6. Adsorption isotherms

Adsorption isotherm is a vital criterion to elucidate the maximum mono layer adsorption capacity and the nature of adsorbent. The equilibrium adsorption isotherms data obtained for three different sets of temperature (25°C, 35°C,and 45°C) using 1 g/L of adsorbent and a pH of 6.7. The experimental data set applied to the linearized form of Langmuir and Freundlich isotherms models Eqns. (6) and (7), respectively [10,32].

$$\frac{C_e}{q_e} = \frac{C_e}{q_m} + \frac{1}{q_m k_L} \tag{6}$$

$$\log(q_e) = \log(k_F) + \frac{1}{n}\log(C_e) \tag{7}$$

where q_e and C_e are amounts of MB adsorbed (mg/g) and MB concentration (mg/l) at equilibrium. k_L (L/mg) and q_m(mg/g) represent the Langmuir constant and maximum adsorption capacity for the formation of a mono layer. K_F (mg/g) and n represent the Freundlich constant and intensity/energy of adsorption process. The plot of Langmuir isotherms model showed good linearity compare to the Freundlich isotherm model for all examined temperature (Figs. 5a and 5b). Moreover, higher values of coefficient of determination (r^2 = 0.997–0.999) also confirmed that the Langmuir isotherms model best suited for the adsorption of MB dye onto graphene monolith (Table 3). These results suggested that binding/adsorptive sites uniformly distributed on the surface of the monolith adsorbent, and the adsorption of MB occurred through the monolayer type adsorption process. The maximum adsorption capacity (q_m) of MB adsorption was in order of 50.76 mg/g (25°C) < 51.55 mg/g (35°C) < 52.08 mg/g (45°C). The observed maximum adsorption capacity (i.e., 50.76 mg/g at 25°C) of graphene monolith showed much higher MB removal efficiency compare to that of powder type reduced graphene, carbon nanotubes, activated carbon and magnetic graphene adsorbents (Table 4). The separation factor (R_L) is an important characteristic of the Langmuir isotherm model to determine the nature of the Langmuir adsorption isotherm model. For example, irreversible (R_L = 0), linear (R_L = 1), favorable (0 < R_L < 1) and unfavorable (R_L > 1)adsorption process [8]. The following equation can estimate the value of R_L:

$$R_L = \frac{1}{1 + K_L C_o} \tag{8}$$

where C_o is the initial concentration of MB dye (mg/l) and K_L is the constant related to the free energy of adsorption. Fig. 5c shows the value of separation factor (R_L) and distri-

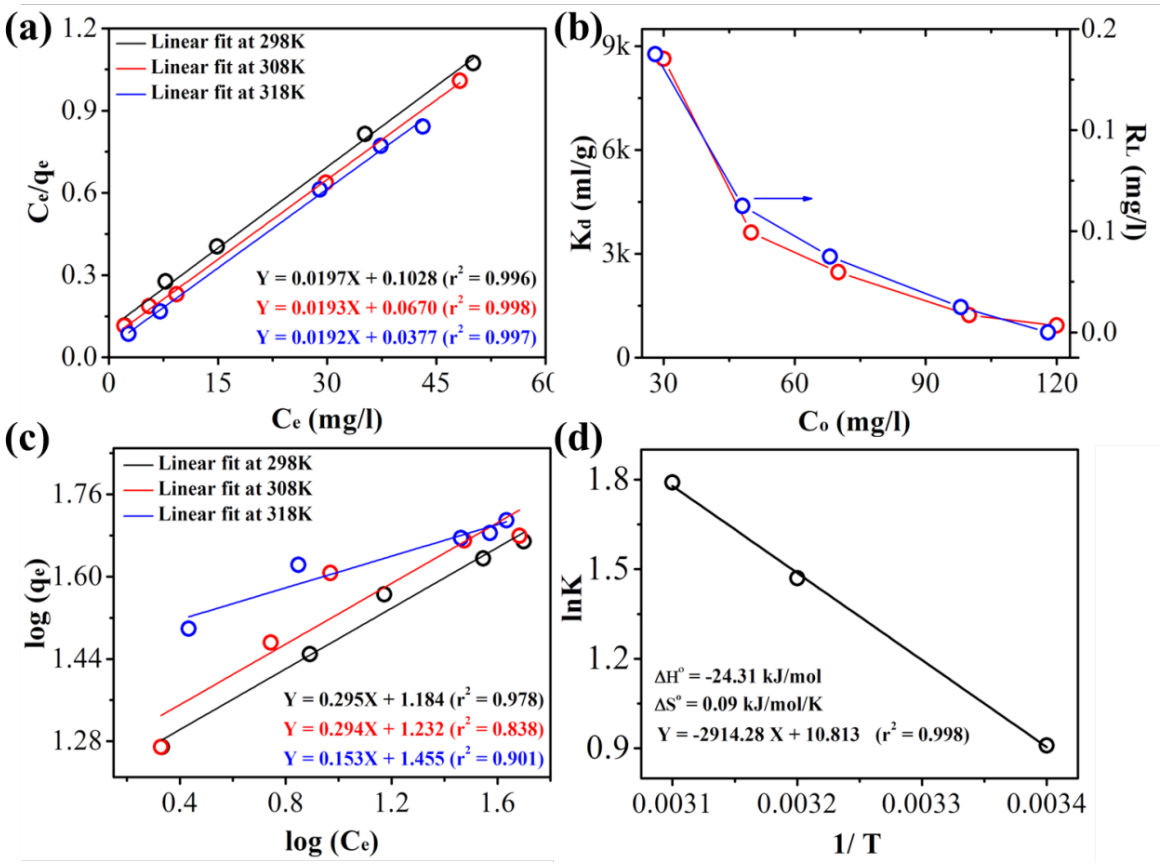

Fig. 5. Langmuir isotherms model (a), Freundlich isotherms model (b), separation factor (R_L) and distribution factor (K_d) (c) and vent Hoff's plot (d) for MB removal.

bution constant (K_d) as a function of the studied concentration range of MB dye. It can be seen that the value of R_L was found to be between 0 and 1 for MB concentration of 30–90 mg/l, indicated that the removal MB dye using graphene monolith was a favorable adsorption process.

3.7. Adsorption thermodynamics

Adsorption of MB dye using graphene monolith further investigated under the influence of operating temperatures (e.g.,298 K, 308 K and 318 K). The experimental data were used to estimate the thermodynamic parameters such as

Table 3
Equilibrium adsorption isotherms parameters for the removal MB dye

Temperature	Freundlich isotherm model			Langmuir isotherm model		
	k_F (mg/g)	n_f	r²	k_L (L/mg)	q_m (mg/g)	r²
25°C	15.297	3.39	0.984	0.191	50.76	0.997
35°C	17.096	3.39	0.879	0.289	51.55	0.999
45°C	28.523	6.98	0.9258	0.509	52.08	0.998

Table 4
Comparative removal capacity of monolith adsorbent for MB dye

Adsorbents	Adsorption capacity (mg/g)	Reference
3D graphene hydrogel	7.85	[23]
Exfoliated graphene oxide	17.30	[33]
Fe_3O_4 nanoparticles	33.2	[34]
Surface modified tamarind seeds carbon	34.48	[8]
Reduced graphene oxide-ferrite hybrids	34.7	[16]
Carrageenan/graphene /Ag composite	39.7	[19]
Magnetic chitosan grafted graphene oxide	43.50	[17]
Graphene / magnetite composite	43.80	[15]
Fe_3O_4/ Graphene	45.30	[20]
Carbon nanotubes	46.20	[35]
Graphene monolith	50.76	This work
Sawdust based activated carbon	58.14	[7]
Titanium dioxide nanotube	57.14	[36]
Graphene/luffa sponge	63.32	[24]

Gibbs free energy, enthalpy and entropy changes using thermodynamics Eqs. (9) and (10), respectively [37].

$$\Delta G^o = -RT\ln(k_L) \tag{9}$$

$$\ln(k_L) = \frac{\Delta S^o}{R} - \frac{\Delta H^o}{RT} \tag{10}$$

where T and R represent the absolute temperature in Kelvin (K) and the constant of universal gas (8.314 J/mol/K). K_L represents the Langmuir isotherm constant. ΔG° (kJ/mol), ΔH° (kJ/ mol) and ΔS° (kJ/ mol/ K) represent the change in Gibbs free energy, enthalpy and entropy respectively. The thermo dynamics parameters listed in Table 5 obtained from the slope and intercept of ln K vs. 1/T. Fig. 5d shows the best linear fit for MB adsorption thermodynamics data (r^2 = 0.998). The negative value of ΔG° showed that adsorption of MB onto graphene monolith was a spontaneous and feasible process. The ΔG° value found to be more negative upon increasing the operating temperature from 298 to 318 K, indicating that removal of MB dye is more accessible at a higher temperature. The negative value of ΔH° indicates that adsorption of MB onto graphene monolith was an exothermic process. The magnitude of ΔH° value gives essential information about the adsorption mechanism such as physical (ΔH° < 80 kJ/mol) /or chemical (80–400 kJ/mol) adsorption. The magnitude of ΔH° was found to be –24.31 kJ/mol, indicated that removal of MB was a physical adsorption process. The positive value of ΔS° showed strong adsorption affinity of MB dye toward graphene monolith. Taking together, thermodynamics results indicate that removal of MB using graphene monolith was an efficient adsorption process.

Table 5
Thermodynamics parameters for the removal MB dye

Temperature	ΔG°(kJ/mol)	ΔH°(kJ/mol)	ΔS°(kJ/ mol/ K)
298 K	–2.569	–24.31	0.090
308 K	–3.471	–	–
318 K	–4.373	–	–

3.8. Adsorption mechanism

The surface chemistry of the adsorbent controls the adsorption of adsorbate. Fig. 6a shows that solution pH had a significant effect on the removal of MB dye. The monolith adsorbent showed an increased in MB removal efficiency from 65 to 98% upon changing the system pH from acidic to alkaline and reached at highest value (>99%) at pH = 10–12. This result indicates that the surface charge of the monolith actively controlled the removal of MB dye (PK_a = 3.8) [2] via electrostatic attraction/ repulsion process. This speculation further confirmed by the measurement of zero points of charge (ZPC) of monolith surface. The pH_{ZPC} value of graphene monolith was found to be ≅ 4.0, which is well accord with reported value of graphene-based adsorbent [38,39]. Hence, the surface of the monolith had nega-

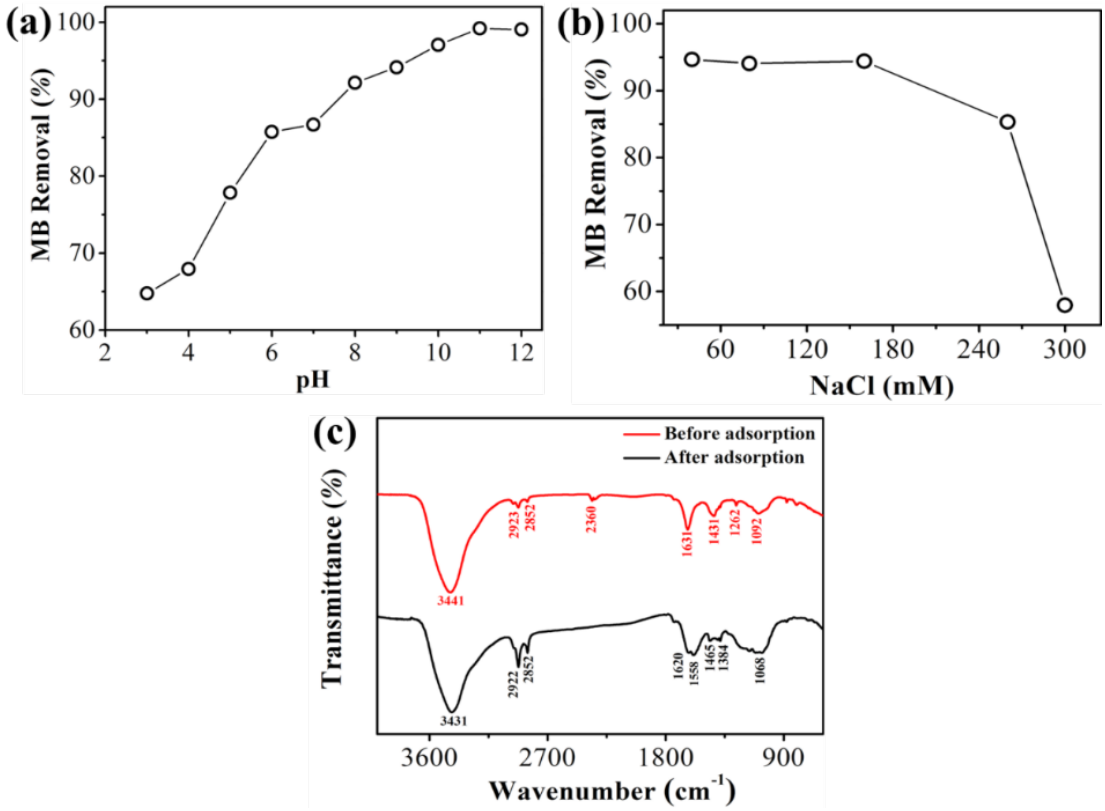

Fig. 6. Effect of pH (a), effect of NaCl concentration (b), and FTIR spectra of monolith before (red spectrum) and after MB adsorption (black spectrum) (c).

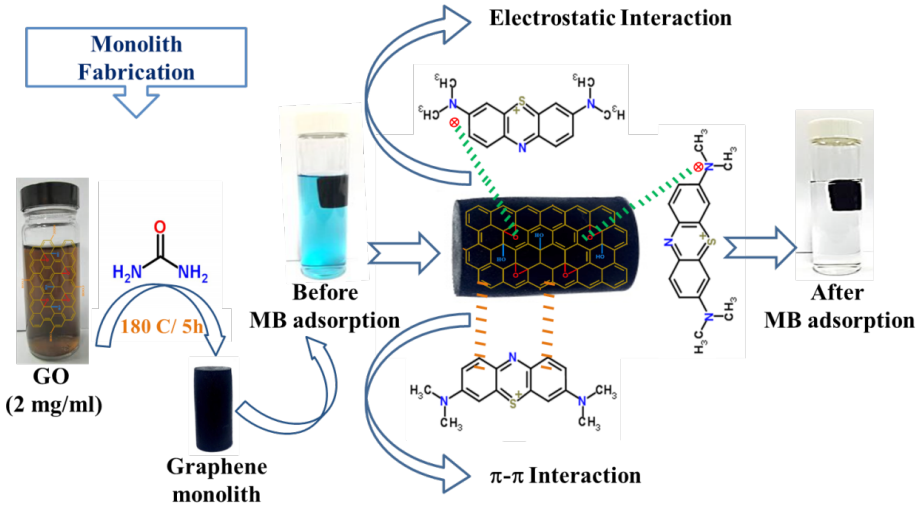

Fig. 7. Fabrication (left), and proposed adsorption mechanisms of MB removal using graphene monolith (right).

tive charges above pH_{ZPC} and positive charges below this pH_{ZPC}. Therefore, at pH > pH_{ZPC} and pH > PK_a the monolith showed greatest removal efficiency for cationic dye MB. It can be seen that 65% of MB removal could achieve under acidic conditions (e.g., pH = 3). Given that, also indicates the contribution of π-π bonding interaction between the aromatic domains of graphene monolith and MB molecules.

The improvement in removal capacity of MB under neutral conditions (pH = 6.8–7.2) was attributed to the deportation of the monolith surface. Further investigations have been made under the effect of sodium chloride concentrations at neutral pH condition. It can be seen that removal of MB remains higher (i.e., 95%) in the concentration range of 160 mM, than tend to decline (Fig. 6b), indicating that an excess of positively charged sodium ions forms electrostatic repulsion with cationic MB molecules for the same binding sites of the monolith. To further probe the interaction of MB dye with graphene monolith, The FTIR spectra of monolith were analyzed before and after adsorption of MB dye (Fig. 6c). As expected, the spectrum of monolith exhibited notable changes after adsorption of MB compares to fresh monolith surface. For example, appearance of the new peak located at 1558 cm^{-1} and shifting of OH band (i.e., from 3441 to 3431 cm^{-1}), C=C/C-N band (from 1631 to 1620 cm^{-1}) and C-O band (from 1092 to 1068 cm^{-1}). These results confirmed the contribution of following MB adsorption mechanisms: (1) the much shifting of oxygen-containing bands indicates the electrostatic interaction (e.g., hydrogen bonding) between monolith surface and amines group of cationic dye MB, and (2) Both, the appearance of the new band at 1558 cm^{-1} and shifting of C=C bands are indicating the vital of role π-π staking interaction between the aromatic ring of graphene and MB molecules [40]. Based on the above discussion, interaction mechanisms of MB removal have been proposed in Fig. 7.

4. Conclusions

In summary, the monolithic form of graphene with tailored macroscopic dimensions can be assembled using urea assisted self-assembly protocols. The fabricated material was characterized and employed as an adsorbent for the removal of MB dye. Complete removal of MB (>99%) can achieve under optimum conditions (e.g., alkaline pH, 160 mM of salt and 1 g/L adsorbent dose at 25°C). The adsorption data analyzed for pseudo-second-order kinetics, pseudo-second-order kinetics, and intra particle diffusion kinetics models. The correlation coefficient demonstrated that dynamics of pseudo-second-order model adequately describes the rate kinetics for MB removal on the monolith. Intra particle diffusion kinetics model showed that surface layer and pore diffusion were rate limiting process. Adsorptive removal of MB onto graphene monolith showed excellent fits to Langmuir isotherm model and found to favorable adsorption process. The sorption capacity (mg/g) was better/comparable to other graphene-based adsorbent (Table 4). Thermodynamics result indicated that the investigated system was favorable, spontaneous and exothermic adsorption process. Electrostatic and π-π staking interactions were identified as significant interaction process for MB dye removal. Overall results demonstrated that removal of MB using graphene monolith provides a promising alternative with no environmental concerns.

Acknowledgments

This research work financially supported by joint research program of national natural science foundation, P.R China (U1660107), Textile light application and basic research, P.R China (J201503), and specialized research funds for doctoral program and senior education in P.R China (20130075110006).

References

[1] P.S. Kumar, S.J. Varjani, S. Suganya, Treatment of dye wastewater using an ultrasonic aided nanoparticle stacked activated carbon: Kinetic and isotherm modelling, Bioresour. Technol., 250 (2018) 716–722.

[2] X. He, K.B. Male, P.N. Nesterenko, D. Brabazon, B. Paull, J.H.T. Luong, Adsorption and desorption of methylene blue on porous carbon monoliths and nanocrystalline cellulose, ACS Appl. Mater. Interfaces, 5 (2013) 8796–8804.
[3] J. Goscianska, M. Marciniak, R. Pietrzak, Mesoporous carbons modified with lanthanum(III) chloride for methyl orange adsorption, Chem. Eng. J., 247 (2014) 258–264.
[4] P. Zhang, T. Wang, G. Qian, D. Wu, R.L. Frost, Removal of methyl orange from aqueous solutions through adsorption by calcium aluminate hydrates, J. Colloid Interface Sci., 426 (2014) 44–47.
[5] M. Anbia, S.A. Hariri, Removal of methylene blue from aqueous solution using nanoporous SBA-3, Desalination, 261 (2010) 61–66.
[6] P. S. Kumar, S. Ramalingam, C. Senthamarai, M. Niranjanaa, P. Vijayalakshmi, S. Sivanesan, Adsorption of dye from aqueous solution by cashew nut shell: Studies on equilibrium isotherm, kinetics and thermodynamics of interactions, Desalination, 261 (2010) 52–60.
[7] S. Suganya, P.S. Kumar, A. Saravanan, P.S. Rajan, C. Ravikumar, Computation of adsorption parameters for the removal of dye from wastewater by microwave assisted sawdust: Theoretical and experimental analysis, Environ. Toxicol. Pharmacol., 50 (2017) 45–57.
[8] P.S. Kumar, R. Sivaranjanee, U. Vinothini, M. Raghavi, K. Rajasekar, K. Ramakrishnan, Adsorption of dye onto raw and surface modified tamarind seeds: isotherms, process design, kinetics and mechanism, Desal. Water Treat., 52 (2014) 2620–2633.
[9] S. Suganya, P.S. Kumar, Kinetic and thermodynamic analysis for the redemption of effluents containing Solo chrome Black T onto powdered activated carbon: A validation of new solid-liquid phase equilibrium model, J. Molec. Liq., 259 (2018) 88–101.
[10] V. Tharaneedhar, P.S. Kumar, A. Saravanan, C. Ravikumar, V. Jaikumar, Prediction and interpretation of adsorption parameters for the sequestration of methylene blue dye from aqueous solution using microwave assisted corncob activated carbon, Sustain. Mater. Technol., 11 (2017) 1–11.
[11] S. Wang, H. Sun, H.M. Ang, M.O. Tadé, Adsorptive remediation of environmental pollutants using novel graphene-based nanomaterials, Chem. Eng. J., 226 (2013) 336–347.
[12] P.S. Kumar, J. Pavithra, S. Suriya, M. Ramesh, K.A. Kumar, Sargassum wightii, a marine alga is the source for the production of algal oil, bio-oil, and application in the dye wastewater treatment, Desal. Water Treat., 55 (2015) 1342–1358.
[13] A. Hussain, J. Li, J. Wang, F. Xue, Y. Chen, T. Bin Aftab, D. Li, Hybrid monolith of graphene/TEMPO-oxidized cellulose nanofiber as mechanically robust, highly functional, and recyclable adsorbent of methylene blue dye, J. Nanomater., 2018 (2018) 12.
[14] J. Zhao, W. Ren, H.-M. Cheng, Graphene sponge for efficient and repeatable adsorption and desorption of water contaminations, J. Mater. Chem., 22 (2012) 20197–20202.
[15] L. Ai, C. Zhang, Z. Chen, Removal of methylene blue from aqueous solution by a solvo thermal-synthesized graphene/magnetite composite, J. Hazard. Mater., 192 (2011) 1515–1524.
[16] S. Bai, X. Shen, X. Zhong, Y. Liu, G. Zhu, X. Xu, K. Chen, One-pot solvo thermal preparation of magnetic reduced graphene oxide-ferrite hybrids for organic dye removal, Carbon., 50 (2012) 2337–2346.
[17] L. Fan, C. Luo, X. Li, F. Lu, H. Qiu, M. Sun, Fabrication of novel magnetic chitosan grafted with graphene oxide to enhance adsorption properties for methyl blue, J. Hazard. Mater., 215–216 (2012) 272–279.
[18] G.Z. Kyzas, E.A. Deliyanni, K.A. Matis, Graphene oxide and its application as an adsorbent for wastewater treatment, J. Chem. Technol. Biotechnol., 89 (2014) 196–205.
[19] B.Y. Zhenga, J. Yanga, R. Yanga, A. Wangc, B. Dengb, F. Penga, Y. Pengd, L. Hee, L. Fua, Novel carrageen an/reduced graphene gxide/Ag composite as adsorbent for removal methylene blue from aqueous solution., Digest J. Nanomater. Biostruct., 10 (2015) 349–357.
[20] Y. Yao, S. Miao, S. Liu, L.P. Ma, H. Sun, S. Wang, Synthesis, characterization, and adsorption properties of magnetic Fe_3O_4@ graphene nanocomposite, Chem. Eng. J., 184 (2012) 326–332.
[21] W. Wan, R. Zhang, W. Li, H. Liu, Y. Lin, L. Li, Y. Zhou, Graphene-carbon nanotube aero gel as an ultra-light, compressible and recyclable highly efficient absorbent for oil and dyes, Environ. Sci. Nano., 3 (2016) 107–113.
[22] H. Bi, X. Xie, K. Yin, Y. Zhou, S. Wan, L. He, F. Xu, F. Banhart, L. Sun, R.S. Ruoff, Graphene: spongy graphene as a highly efficient and recyclable sorbent for oils and organic solvents, Adv. Funct. Mater., 22 (2012) 4401–4401.
[23] J.N. Tiwari, K. Mahesh, N.H. Le, K.C. Kemp, R. Timilsina, R.N. Tiwari, K.S. Kim, Reduced graphene oxide-based hydro gels for the efficient capture of dye pollutants from aqueous solutions, Carbon., 56 (2013) 173–182.
[24] S. Li, M. Tao, Y. Xie, Reduced graphene oxide modified luffa sponge as a biocomposite adsorbent for effective removal of cationic dyes from aqueous solution, Desal. Water Treat., 57 (2016) 20049–20057.
[25] Y.C. Shi, A.J. Wang, X.L. Wu, J.R. Chen, J.J. Feng, Green-assembly of three-dimensional porous graphene hydro gels for efficient removal of organic dyes, J. Colloid Interface Sci., 484 (2016) 254–262.
[26] Y. Cheng, P. Xu, W. Zeng, C. Ling, S. Zhao, K. Liao, Y. Sun, A. Zhou, Highly hydrophobic and ultralight graphene aero gel as high efficiency oil absorbent material, J. Environ. Chem. Eng., 5 (2017) 1957–1963.
[27] F. Wang, Y. Wang, W. Zhan, S. Yu, W. Zhong, G. Sui, X. Yang, Facile synthesis of ultra-light graphene aerogels with super absorption capability for organic solvents and strain-sensitive electrical conductivity, Chem. Eng. J., 320 (2017) 539–548.
[28] W.S. Hummers, R.E. Offeman, Preparation of graphitic oxide, J. Am. Chem. Soc., 80 (1958) 1339–1339.
[29] C.C. Ji, M.W. Xu, S.J. Bao, C.J. Cai, Z.J. Lu, H. Chai, F. Yang, H. Wei, Self-assembly of three-dimensional interconnected graphene-based aerogels and its application in super capacitors, J. Colloid Interface Sci., 407 (2013) 416–424.
[30] Y. Wang, B. Fugetsu, I. Sakata, M. Terrones, M. Endo, M. Dresselhaus, Morphology-controlled fabrication of a three-dimensional mesoporous poly(vinyl alcohol) monolith through the incorporation of graphene oxide, Carbon, 98 (2016) 334–342.
[31] J.A. Weber, J.C. Morris, Kinetics of adsorption on carbon solution., J. Sanit. Eng. Div. Am. Soc. Civ. Eng., 89(31–59) (1963) 89 31–59.
[32] I. Langmuir, The adsorption of gases on plane surfaces of glass, mica and platinum., J. Am. Chem. Soc., 40 (1981) 1361–1403.
[33] G.K. Ramesha, A. Vijaya Kumara, H.B. Muralidhara, S. Sampath, Graphene and graphene oxide as effective adsorbents toward anionic and cationic dyes, J. Colloid Interface Sci., 361 (2011) 270–277.
[34] M. Ghaedi, S. Hajjati, Z. Mahmudi, I. Tyagi, S. Agarwal, A. Maity, V.K. Gupta, Modeling of competitive ultrasonic assisted removal of the dyes Methylene blue and Safranin-O using Fe_3O_4 nanoparticles, Chem. Eng. J., 268 (2015) 28–37.
[35] L. Ai, J. Jiang, Removal of methylene blue from aqueous solution with self-assembled cylindrical graphene–carbon nanotube hybrid, Chem. Eng. J., 192 (2012) 156–163.
[36] T.S. Natarajan, H.C. Bajaj, R.J. Tayade, Preferential adsorption behavior of methylene blue dye onto surface hydroxyl group enriched TiO_2 nanotube and its photo catalytic regeneration, J. Colloid Interface Sci., 433 (2014) 104–114.
[37] W.L. Haochun Shi, L. Zhong, C. Xu, Methylene blue adsorption from aqueous solution by magnetic cellulose/graphene oxide composite: Equilibrium, Kinetics, and Thermodynamics, Indus. Eng. Chem. Res., 53 (2014) 1108–1118.
[38] X.F. Sun, B.B. Guo, L. He, P.F. Xia, S.G. Wang, Electrically accelerated removal of organic pollutants by a three-dimensional graphene aerogel, AIChE . J., 62 (2016) 2154–2162.
[39] Y. Bian, Z.Y. Bian, J.X. Zhang, A.Z. Ding, S.L. Liu, H. Wang, Effect of the oxygen-containing functional group of graphene oxide on the aqueous cadmium ions removal, Appl. Surf. Sci., 329 (2015) 269–275.
[40] J. Fu, Z. Chen, M. Wang, S. Liu, J. Zhang, J. Zhang, R. Han, Q. Xu, Adsorption of methylene blue by a high-efficiency adsorbent (polydopamine micro spheres): Kinetics, isotherm, thermodynamics and mechanism analysis, Chem. Eng. J., 259 (2015) 53–61.